Results from a Low-Energy Analysis of the CDMS II Germanium Data

Z. Ahmed,[1] D. S. Akerib,[2] S. Arrenberg,[19] C. N. Bailey,[2] D. Balakishiyeva,[17] L. Baudis,[19] D. A. Bauer,[3] P. L. Brink,[7] T. Bruch,[19] R. Bunker,[15] B. Cabrera,[11] D. O. Caldwell,[15] J. Cooley,[10] E. do Couto e Silva,[7] P. Cushman,[18] M. Daal,[14] F. DeJongh,[3] P. Di Stefano,[6] M. R. Dragowsky,[2] L. Duong,[18] S. Fallows,[18] E. Figueroa-Feliciano,[5] J. Filippini,[1] J. Fox,[6] M. Fritts,[18] S. R. Golwala,[1] J. Hall,[3] R. Hennings-Yeomans,[2] S. A. Hertel,[5] D. Holmgren,[3] L. Hsu,[3] M. E. Huber,[16] O. Kamaev,[18] M. Kiveni,[12] M. Kos,[12] S. W. Leman,[5] S. Liu,[6] R. Mahapatra,[13] V. Mandic,[18] K. A. McCarthy,[5] N. Mirabolfathi,[14] D. Moore,[1,*] H. Nelson,[15] R. W. Ogburn,[11] A. Phipps,[14] M. Pyle,[11] X. Qiu,[18] E. Ramberg,[3] W. Rau,[6] A. Reisetter,[18,8] R. Resch,[7] T. Saab,[17] B. Sadoulet,[4,14] J. Sander,[15] R. W. Schnee,[12] D. N. Seitz,[14] B. Serfass,[14] K. M. Sundqvist,[14] M. Tarka,[19] P. Wikus,[5] S. Yellin,[11,15] J. Yoo,[3] B. A. Young,[9] and J. Zhang[18]

(CDMS Collaboration)

[1]Division of Physics, Mathematics & Astronomy, California Institute of Technology, Pasadena, California 91125, USA
[2]Department of Physics, Case Western Reserve University, Cleveland, Ohio 44106, USA
[3]Fermi National Accelerator Laboratory, Batavia, Illinois 60510, USA
[4]Lawrence Berkeley National Laboratory, Berkeley, California 94720, USA
[5]Department of Physics, Massachusetts Institute of Technology, Cambridge, Massachusetts 02139, USA
[6]Department of Physics, Queen's University, Kingston, ON, Canada, K7L 3N6
[7]SLAC National Accelerator Laboratory/KIPAC, Menlo Park, California 94025, USA
[8]Department of Physics, St. Olaf College, Northfield, Minnesota 55057 USA
[9]Department of Physics, Santa Clara University, Santa Clara, California 95053, USA
[10]Department of Physics, Southern Methodist University, Dallas, Texas 75275, USA
[11]Department of Physics, Stanford University, Stanford, California 94305, USA
[12]Department of Physics, Syracuse University, Syracuse, New York 13244, USA
[13]Department of Physics, Texas A & M University, College Station, Texas 77843, USA
[14]Department of Physics, University of California, Berkeley, California 94720, USA
[15]Department of Physics, University of California, Santa Barbara, California 93106, USA
[16]Departments of Physics & Electrical Engineering, University of Colorado Denver, Denver, Colorado 80217, USA
[17]Department of Physics, University of Florida, Gainesville, Florida 32611, USA
[18]School of Physics & Astronomy, University of Minnesota, Minneapolis, Minnesota 55455, USA
[19]Physics Institute, University of Zürich, Winterthurerstrasse 190, CH-8057, Switzerland

We report results from a reanalysis of data from the Cryogenic Dark Matter Search (CDMS II) experiment at the Soudan Underground Laboratory. Data taken between October 2006 and September 2008 using eight germanium detectors are reanalyzed with a lowered, 2 keV recoil-energy threshold, to give increased sensitivity to interactions from weakly interacting massive particles (WIMPs) with masses below ~ 10 GeV/c^2. This analysis provides stronger constraints than previous CDMS II results for WIMP masses below 9 GeV/c^2 and excludes parameter space associated with possible low-mass WIMP signals from the DAMA/LIBRA and CoGeNT experiments.

A convergence of astrophysical observations indicates that $\sim 80\%$ of the matter in the Universe is in the form of nonbaryonic, nonluminous dark matter [1]. Weakly interacting massive particles (WIMPs) [2], with masses from a few GeV/c^2 to a few TeV/c^2, form a well-motivated class of candidates for this dark matter [1,3]. If WIMPs account for the dark matter, they may be detectable through their elastic scattering with nuclei in terrestrial detectors [4].

Although many models of physics beyond the standard model provide WIMP candidates, supersymmetric (SUSY) models where the lightest superpartner is a cosmologically stable WIMP are among the most popular [1,3]. In the minimal supersymmetric standard model (MSSM), WIMPs with masses $\lesssim 40$ GeV/c^2 are generally disfavored by accelerator constraints (e.g., [5]). Interest in lower-mass WIMPs has been renewed by recent results from the DAMA/LIBRA [6] and CoGeNT [7] experiments, which have been interpreted in terms of elastic scatters from a WIMP with mass ~ 10 GeV/c^2 and cross-section $\sim 10^{-40}$ cm^2 [8,9]. Although it is difficult to accommodate a WIMP with these properties in the MSSM [10], alternate models avoid existing constraints (e.g., [11]).

The CDMS II experiment attempts to identify nuclear recoils from WIMPs in an array of particle detectors by

measuring both the ionization and nonequilibrium phonons created by each particle interaction. Backgrounds can be rejected on an event-by-event basis since they primarily scatter from electrons in the detector, depositing significantly more ionization than a nuclear recoil of the same energy. Previous analyses of CDMS II data [12] imposed a recoil-energy threshold of 10 keV to maintain sufficient rejection of electron recoils that only ~0.5 background events would be expected in the signal region. At lower energies, the discrimination between nuclear and electron recoils degrades, leading to higher expected backgrounds. Since WIMPs with masses <10 GeV/c^2 primarily produce <10 keV recoils, this analysis lowers the recoil-energy threshold to 2 keV, comparable to the hardware trigger threshold. This lower energy threshold increases sensitivity to low-mass WIMPs at the cost of significant acceptance of backgrounds.

The data analyzed here were collected using all 30 Z-sensitive Ionization and Phonon (ZIP) detectors installed at the Soudan Underground Laboratory [12,13]. The detector array consisted of 19 Ge (~ 230 g each) and 11 Si (~ 105 g each) detectors, each a disk ~ 10 mm thick and 76 mm in diameter. Each detector was instrumented with four phonon sensors on one face and two concentric charge electrodes on the opposite face. A small electric field (3–4 V/cm) was applied across the detectors to extract charge carriers created by particle interactions. The detectors were arranged in five "towers," and are identified by their tower number ($T1$–$T5$) and by their ordering within the tower ($Z1$–$Z6$). The entire array was cooled to $\lesssim 50$ mK and surrounded by passive lead and polyethylene shielding. An outer plastic scintillator veto was used to identify showers containing cosmogenic muons which were not shielded by the rock overburden above the Soudan laboratory (2090 meters water equivalent).

The data were taken during six data runs from October 2006 to September 2008 [12]. Only the eight Ge detectors with the lowest trigger thresholds were used to identify WIMP candidate events since they have the best expected sensitivity to WIMPs with masses from 5–10 GeV/c^2. All 30 detectors were used to veto events that deposited energy in multiple detectors.

Each detector was monitored throughout the data runs and periods of abnormal detector performance were removed [12]. Data taken within 20 days following exposure of the detectors to a neutron calibration source were removed to reduce low-energy electron-recoil backgrounds due to activation of the detectors. The data were randomly divided into two subsets before defining selection criteria at low energy. One subset, consisting of one quarter of the data (the "open" data), was reserved to study backgrounds at low energy and was not used to calculate exclusion limits. The remaining subset totaled 241 kg d raw exposure, after removing the bad data periods described above.

The detector response to electron and nuclear recoils was calibrated by regular exposures of the detectors to γ-ray (^{133}Ba) and neutron (^{252}Cf) sources. The ionization-energy scale was initially calibrated using the 356 keV line from the ^{133}Ba source. The phonon energy was then calibrated by normalizing the phonon-based recoil energy for electron recoils to their mean ionization energy. In contrast to previous analyses, a position-dependent calibration was not applied since position-dependent variations in the reconstructed phonon energies are less significant than noise fluctuations at low energies. Using the observed positions of the 1.3 and 10.4 keV activation lines produced from exposure of the Ge detectors to the ^{252}Cf source, a small rescaling ($\sim 4\%$) was applied to ensure that the recoil-energy scale for electron recoils was not underestimated at the 90% confidence level. For nuclear recoils, the recoil energy was reconstructed from the measured phonon energy alone by subtracting the Neganov-Luke phonon contribution [14] corresponding to the mean ionization measured for nuclear recoils of the same phonon energy from the ^{252}Cf source. The ratio of ionization to recoil energy ("ionization yield") for nuclear recoils was measured down to ~ 4 keV, below which a power-law extrapolation was used.

Candidate events were required to pass basic reconstruction quality cuts similar to the criteria used in previous analyses of these data [12]. Because of the negligible probability of a WIMP interacting more than once in the apparatus, candidates were required to have energies consistent with noise in all but one detector and have no coincident activity in the plastic scintillator veto. They were further required to have ionization signals consistent with noise in the outer charge electrode. The ionization energy was required to be within $(+1.25, -0.5)\sigma$ of the mean ionization energy for nuclear recoils measured from calibration data, which defines the "nuclear-recoil band." This asymmetric band, which has been tightened relative to previous low-energy analyses [15,16], was chosen based on calibration data and the observed low-energy backgrounds in the open data in order to maximize sensitivity to nuclear recoils while limiting leakage from electron recoils and zero-charge events. The recoil-energy range considered for this analysis was 2–100 keV.

The hardware trigger efficiency was determined using events for which at least one other detector triggered, which provide an unbiased selection of events near threshold. The data are well described by an error function, with the mean trigger threshold varying from 1.5–2.5 keV for the eight Ge detectors. Based on the selection criteria above, the signal acceptance was measured using nuclear recoils from the ^{252}Cf calibration data. We calculated the nuclear-recoil band acceptance conservatively by assuming all events with ionization energy $<3\sigma$ above the mean of the distribution were nuclear recoils. In particular, the zero-charge events described below were included,
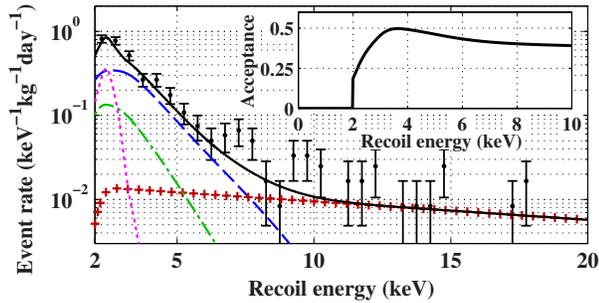
FIG. 1 (color online).   Comparison of the energy spectra for the candidate events and background estimates, co-added over the 8 detectors used in this analysis. The observed event rate (error bars) agrees well with the electron-recoil background estimate (solid line), which is a sum of the contributions from zero-charge events (dashed line), surface events (+), bulk events (dash-dotted line), and the 1.3 keV line (dotted line). The selection efficiencies have been applied to the background estimates for direct comparison with the observed rate, which does not include a correction for the nuclear-recoil acceptance. The inset shows the measured nuclear-recoil acceptance efficiency, averaged over all detectors.

FIG. 2 (color online).   Events in the ionization-yield versus recoil-energy plane for T1Z5. Events within the $(+1.25, -0.5)\sigma$ nuclear-recoil band (solid) are WIMP candidates (large dots). Events outside these bands (small, dark dots) pass all selection criteria except the ionization-energy requirement. The widths of the band edges denote variations between data runs. Events from the ^{252}Cf calibration data are also shown (small, light dots). The recoil-energy scale assumes the ionization signal is consistent with a nuclear recoil, causing electron recoils to be shifted to higher recoil energies and lower yields.

although their rate in the ^{252}Cf calibration data is negligible. The livetime-weighted average of the individual detector selection efficiencies is shown in the inset of Fig. 1, with the largest loss of efficiency coming from the requirement on ionization energy.

The energy spectrum for the candidate events passing all selection cuts is shown in Fig. 1. Although the shape of the observed spectrum is consistent with a WIMP signal, we expect that a significant number of the candidates are due to unrejected electron recoils. Figure 2 shows the distribution of candidates in the ionization-yield versus recoil-energy plane for $T1Z5$. Several populations of events which can leak into the signal region at low energy are apparent. For each population described below, we measure the rate and energy spectrum in sidebands where the contribution from low-mass WIMPs would be negligible, and extrapolate the observed spectrum to lower energies to estimate the leakage. The systematic errors introduced by these extrapolations are potentially large and are difficult to quantify. However, as shown in Fig. 1 and discussed below, these simple extrapolations can plausibly explain all the observed candidates.

Events with ionization energies consistent with noise are seen below the nuclear-recoil band. Most or all of these "zero-charge" events arise from electron recoils near the edge of the detector, where the charge carriers can be completely collected on the cylindrical wall rather than on the readout electrodes. At recoil energies $\gtrsim 10$ keV, these events can be rejected using a phonon-based fiducial-volume cut. At lower energies, reconstruction of the event radius using phonon information is unreliable. To maintain acceptance of low-energy nuclear recoils, some zero-charge events are not rejected at energies $\lesssim 5$ keV where
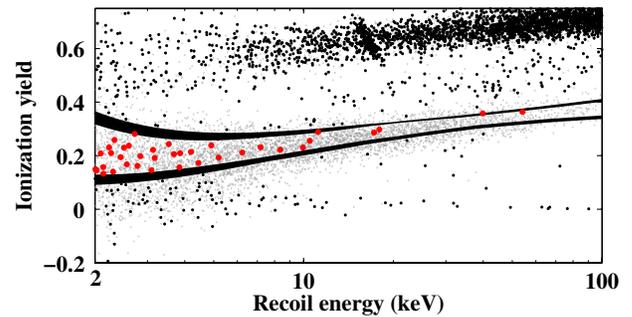
the ionization signal for nuclear recoils becomes comparable to noise. By extrapolating the exponential spectrum observed for zero-charge events above 5 keV, we estimate that they contribute $\sim 50\%$ of the candidate events.

A second source of misidentified electron recoils comes from events interacting near the detector surfaces, where ionization collection may be incomplete. These events are primarily concentrated just above the nuclear-recoil band, with an increased fraction leaking into the signal region at low energies. For recoil energies $\gtrsim 10$ keV, nearly all such surface events can be rejected [12] because they have faster-rising phonon pulses than nuclear recoils in the bulk of the detector. This analysis does not use phonon timing to reject these events since the signal-to-noise is too low for this method to be effective for recoil energies $\lesssim 5$ keV. Extrapolating the exponential spectrum of surface events identified above 10 keV implies that $\sim 15\%$ of the candidates are surface electron recoils.

At recoil energies $\lesssim 5$ keV, the primary ionization-based discrimination breaks down as the ionization signal becomes comparable to noise even for electron recoils with fully collected charge. Extrapolating the roughly constant electron-recoil spectrum observed above 5 keV indicates that $\sim 10\%$ of the observed candidates arise from leakage of this background into the signal region. Just above threshold, there is an additional contribution to the constant electron-recoil spectrum from the 1.3 keV line, which leaks above the 2 keV analysis threshold since our recoil-energy estimate assumes the ionization signal is consistent with a nuclear recoil. The measured intensity of this line at ionization yields above the signal region indicates that the 1.3 keV line accounts for $\sim 10\%$ of the observed candidates. $T1Z5$ has less expected leakage from these fully collected electron-recoil backgrounds than the average detector since it has the best ionization resolution.

These estimates indicate that we can claim no evidence for a WIMP signal. However, since the background model involves sufficient extrapolation that systematic errors are difficult to quantify, we do not subtract backgrounds but instead set upper limits on the allowed WIMP-nucleon scattering cross section by conservatively assuming all observed events could be from WIMPs. Limits are calculated using the high statistics version of Yellin's optimum interval method [17]. Data from multiple detectors are concatenated as described in [16]. This method allows the choice of the most constraining energy interval on the lowest background detector while applying the appropriate statistical penalty for the freedom to choose this interval. The method and the ordering of detectors by position within the tower were specified with no knowledge of the WIMP candidates to avoid bias. For WIMP masses from 5–8 GeV/c^2, the most constraining interval contains events only from $T1Z5$ and has no dependence on the detector ordering used. The standard halo model described in [18] is used, with specific parameters given in [16,19]. The candidate event energies and selection efficiencies for each detector are given in [19].

The limits do not depend strongly on the extrapolation of the ionization yield used at low energies since the Neganov-Luke phonon contribution is small for recoil energies below 4 keV. Conservatively assuming 25% lower ionization yield near threshold would lead to only ~5% weaker limits in the 5–10 GeV/c^2 mass range.

Figure 3 (upper panel) shows the resulting 90% upper confidence limit on the spin-independent WIMP-nucleon scattering cross section. This analysis provides stronger limits than previous CDMS II Ge results for WIMP masses below ~9 GeV/c^2, and excludes parameter space previously excluded only by the XENON10 and XENON100 experiments for a constant extrapolation of the liquid xenon scintillation response for nuclear recoils below 5 keV [20–22]. Our analysis provides stronger constraints than XENON10 and XENON100 below ~7 GeV/c^2 under conservative assumptions for the scintillation response [8,20,23].

Spin-dependent limits on the WIMP-neutron cross section are shown in Fig. 3 (lower panel), using the form factor from [24]. XENON10 constraints, calculated assuming a constant extrapolation of the scintillation response at low energy [23,25], are stronger than these results for WIMP masses above ~7 GeV/c^2.

These results exclude interpretations of the DAMA/LIBRA annual modulation signal in terms of spin-independent elastic scattering of low-mass WIMPs (e.g., [8,22]). We ignore the effect of ion channeling on the DAMA/LIBRA allowed regions since recent analyses indicate channeling should be negligible [22,26]. These results are also incompatible with a low-mass WIMP explanation for the low-energy events seen in CoGeNT [7,8].
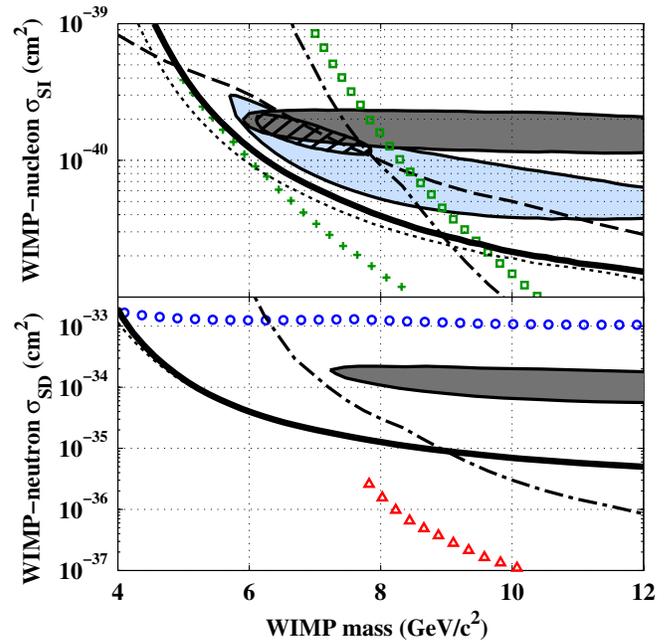

FIG. 3 (color online). Top: comparison of the spin-independent (SI) exclusion limits from these data (solid line) to previous results in the same mass range (all at 90% C.L.). Limits from a low-threshold analysis of the CDMS shallow-site data [16] (dashed line), CDMS II Ge results with a 10 keV threshold [12] (dash-dotted line), recalculated for lower WIMP masses, and XENON100 with constant (+) or decreasing (□) scintillation-efficiency extrapolations at low-energy [20] are also shown. The filled regions indicate possible signal regions from DAMA/LIBRA [6,8] (dark line), CoGeNT (light) [7,8], and a combined fit to the DAMA/LIBRA and CoGeNT data [8] (hatched). Bottom: comparison of the WIMP-neutron spin-dependent (SD) exclusion limits from these data (solid line), CDMS II Ge results with a 10 keV threshold (dash-dotted line), XENON10 [25] (△), and CRESST [27] (○). The filled region denotes the 99.7% C.L. DAMA/LIBRA allowed region for neutron-only scattering [28]. An escape velocity of 544 km/s was used for the CDMS and XENON100 exclusion limits, whereas the other results assume an escape velocity from 600–650 km/s. Using the same halo parameters as assumed for the allowed regions would lead to slightly stronger limits (dotted line).

---

*Corresponding author.
davidm@caltech.edu

[1] G. Bertone, D. Hooper, and J. Silk, Phys. Rep. **405**, 279 (2005).

[2] G. Steigman and M. S. Turner, Nucl. Phys. **B253**, 375 (1985).

[3] G. Jungman, M. Kamionkowski, and K. Griest, Phys. Rep. **267**, 195 (1996).

[4] M. W. Goodman and E. Witten, Phys. Rev. D **31**, 3059 (1985); R. J. Gaitskell, Annu. Rev. Nucl. Part. Sci. **54**, 315 (2004).

[5] E. A. Baltz and P. Gondolo, J. High Energy Phys. 10 (2004) 052; A. Heister et al., Phys. Lett. B **583**, 247 (2004).

[6] R. Bernabei et al. (DAMA/LIBRA), Eur. Phys. J. C **56**, 333 (2008); R. Bernabei et al., ibid. **67**, 39 (2010).

[7] C. E. Aalseth et al. (CoGeNT), arXiv:1002.4703v2 [Phys. Rev. Lett. (to be published)].

[8] D. Hooper et al., Phys. Rev. D **82**, 123509 (2010).

[9] A. L. Fitzpatrick, D. Hooper, and K. M. Zurek, Phys. Rev. D **81**, 115005 (2010); S. Chang et al., J. Cosmol. Astropart. Phys. 08 (2010) 018; S. Andreas et al., Phys. Rev. D **82**, 043522 (2010).

[10] E. Kuflik, A. Pierce, and K. M. Zurek, Phys. Rev. D **81**, 111701 (2010); D. Feldman, Z. Liu, and P. Nath, ibid. **81**, 117701 (2010); D. Hooper and T. Plehn, Phys. Lett. B **562**, 18 (2003).

[11] A. Bottino et al., Phys. Rev. D **69**, 037302 (2004); P. Draper et al., Phys. Rev. Lett. **106**, 121805 (2011); D. Albornoz Vásquez et al., Phys. Rev. D **82**, 115027 (2010);

A. V. Belikov et al., arXiv:1009.0549v1; G. Bélanger et al., J. High Energy Phys. 03 (2004) 012; J. L. Feng, J. Kumar, and L. E. Strigari, Phys. Lett. B **670**, 37 (2008); S. Andreas, T. Hambye, and M. H. G. Tytgat, J. Cosmol. Astropart. Phys. 10 (2008) 034; K. M. Zurek, Phys. Rev. D **79**, 115002 (2009).

[12] Z. Ahmed et al. (CDMS), Phys. Rev. Lett. **102**, 011301 (2009); Science **327**, 1619 (2010).

[13] D. S. Akerib et al. (CDMS), Phys. Rev. D **72**, 052009 (2005).

[14] B. Neganov and V. Trofimov, Otkrytia, Izobreteniya **146**, 215 (1985); P. N. Luke, J. Appl. Phys. **64**, 6858 (1988).

[15] R. W. Ogburn, Ph.D. thesis, Stanford University, 2008.

[16] D. S. Akerib et al. (CDMS), Phys. Rev. D **82**, 122004 (2010).

[17] S. Yellin, Phys. Rev. D **66**, 032005 (2002); arXiv:0709.2701v1.

[18] J. D. Lewin and P. F. Smith, Astropart. Phys. **6**, 87 (1996).

[19] See supplemental material at http://link.aps.org/supplemental/10.1103/PhysRevLett.106.131302.

[20] E. Aprile et al. (XENON100), Phys. Rev. Lett. **105**, 131302 (2010).

[21] P. Sorensen, J. Cosmol. Astropart. Phys. 09 (2010) 033.

[22] C. Savage et al., Phys. Rev. D **83**, 055002 (2011).

[23] J. I. Collar and D. N. McKinsey, arXiv:1005.0838v3.

[24] V. I. Dimitrov, J. Engel, and S. Pittel, Phys. Rev. D **51**, R291 (1995).

[25] J. Angle et al. (XENON10), Phys. Rev. Lett. **101**, 091301 (2008).

[26] N. Bozorgnia, G. B. Gelmini, and P. Gondolo, J. Cosmol. Astropart. Phys. 11 (2010) 019.

[27] G. Angloher et al. (CRESST), Astropart. Phys. **18**, 43 (2002); C. Savage, P. Gondolo, and K. Freese, Phys. Rev. D **70**, 123513 (2004).

[28] C. Savage et al., J. Cosmol. Astropart. Phys. 04 (2009) 010.